Accepted Manuscript

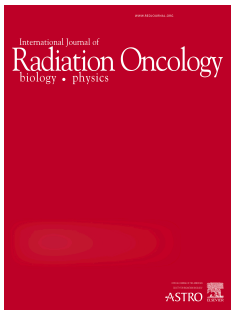

A Roberts Syndrome individual with differential genotoxin sensitivity and a DNA damage response defect

Michael J. McKay, PhD, Jeffery Craig, PhD, Paul Kalitsis, PhD, Sergei Kozlov, PhD, Sandra Verschoor, BSc, Phillip Chen, PhD, Pavel Lobachevsky, PhD, Raja Vasireddy, PhD, Yuqian Yan, PhD, Jacinta Ryan, PhD, George McGillivray, PhD, Ravi Savarirayan, PhD, Martin F. Lavin, PhD, Robert G. Ramsay, PhD, Huiling Xu, PhD

PII: S0360-3016(18)34044-6

DOI: https://doi.org/10.1016/j.ijrobp.2018.11.047

Reference: ROB 25419

To appear in: *International Journal of Radiation Oncology • Biology • Physics*

Received Date: 18 August 2018

Revised Date: 14 November 2018

Accepted Date: 23 November 2018

Please cite this article as: McKay MJ, Craig J, Kalitsis P, Kozlov S, Verschoor S, Chen P, Lobachevsky P, Vasireddy R, Yan Y, Ryan J, McGillivray G, Savarirayan R, Lavin MF, Ramsay RG, Xu H, A Roberts Syndrome individual with differential genotoxin sensitivity and a DNA damage response defect, *International Journal of Radiation Oncology • Biology • Physics* (2018), doi: https://doi.org/10.1016/j.ijrobp.2018.11.047.

A Roberts Syndrome individual with differential genotoxin sensitivity and a DNA damage response defect

Running title: Roberts and DNA damage response

Michael J. McKay*, PhD
Olivia Newton-John Cancer Research Institute and Austin Health, Heidelberg, Victoria 3084, Australia
Latrobe University, Plenty Road, Bundoora, Victoria 3086, Australia
Jeffery Craig*, PhD
Murdoch Children's Research Institute, Royal Children's Hospital, Parkville, Victoria 3052, Australia
Paul Kalitsis*, PhD
Murdoch Children's Research Institute, Royal Children's Hospital, Parkville, Victoria 3052, Australia
Sergei Kozlov, PhD
University of Queensland Centre for Clinical Research, Royal Brisbane & Women's Hospital Campus, Herston, Queensland 4029, Australia
Sandra Verschoor, BSc
Cancer Research Division, Peter MacCallum Cancer Centre, East Melbourne, Victoria 3002, Australia
Phillip Chen, PhD
University of Queensland Centre for Clinical Research, Royal Brisbane & Women's Hospital Campus, Herston, Queensland 4029, Australia
Pavel Lobachevsky, PhD
Cancer Research Division, Peter MacCallum Cancer Centre, East Melbourne, Victoria 3002, Australia
Raja Vasireddy, PhD
Cancer Research Division, Peter MacCallum Cancer Centre, East Melbourne, Victoria 3002, Australia
Yuqian Yan, PhD
Cancer Research Division, Peter MacCallum Cancer Centre, East Melbourne, Victoria 3002, Australia
Jacinta Ryan, PhD
School of Medicine, Flinders University, Adelaide, South Australia 5001, Australia
Victorian Clinical Genetics Services, Murdoch Children's Research Institute, Parkville, Victoria 3052, Australia
George McGillivray, PhD
Victorian Clinical Genetics Services, Murdoch Children's Research Institute, Parkville, Victoria 3052, Australia
Ravi Savarirayan, PhD
Victorian Clinical Genetics Services, Murdoch Children's Research Institute, Parkville, Victoria 3052, Australia
Martin F Lavin, PhD
University of Queensland Centre for Clinical Research, Royal Brisbane & Women's Hospital Campus, Herston, Queensland 4029, Australia
Robert G Ramsay, PhD

Cancer Research Division, Peter MacCallum Cancer Centre, East Melbourne, Victoria 3002, Australia
Sir Peter MacCallum Department of Oncology, Faculty of Medicine, Dentistry and Health Sciences, The University of Melbourne, Parkville, Victoria 3010, Australia
Huiling Xu, PhD
Cancer Research Division, Peter MacCallum Cancer Centre, East Melbourne, Victoria 3002, Australia
Clinical Pathology, Faculty of Medicine, Dentistry and Health Sciences, The University of Melbourne, Parkville, Victoria 3010, Australia

Corresponding author
Dr Huiling Xu
305 Grattan Street
Melbourne, Victoria
3000 Australia
Phone +61 3 85598432
Email huiling.xu@petermac.org

* Equal 1st author

Authors have no conflicts of interest

The study is founded by the NHMRC of Australia for Project Grants

ACKNOWLEDGEMENT

We thank the NHMRC of Australia for Project Grants to HX/MJM/RGR/JC/PK/MFL and SK. We acknowledge the microscopy core at the Peter MacCallum Cancer Centre.

SUMMARY

Purpose: Roberts Syndrome (RBS) is a rare recessively-transmitted developmental disorder characterized by growth retardation, craniofacial abnormalities and truncation of limbs. All affected individuals to date have mutations in the *ESCO2* (Establishment of cohesion 2) gene, a key regulator of the cohesin complex, which is involved in sister chromatid cohesion and DNA double-strand break (dsb) repair. Here we characterize DNA damage responses (DDRs) for the first time in a RBS-affected family.

Methods and Materials: Lymphoblastoid cell lines (LCLs) were established from an RBS family, including the proband, and parents carrying ESCO2 mutations. Various DDR assays were performed on these cells, including clonogenic, chromosome break and apoptosis assays, checkpoint activation indicators and measures of DNA breakage and repair.

Results: Cells derived from the RBS-affected individual showed sensitivity to ionizing radiation (IR) and Mitomycin C (MMC) -induced DNA damage. In this *ESCO2* compound heterozygote, other DNA damage responses were also defective, including enhanced IR-induced clastogenicity and apoptosis, increased DNA dsb induction and a reduced capacity for repairing IR -induced DNA dsbs as measured by γ-H2AX foci and the comet assay.

Conclusions: in addition to its developmental features, RBS can be, like ataxia telangiectasia, considered a DNA damage response-defective syndrome, which contributes to its cellular, molecular and clinical phenotype.

INTRODUCTION

Roberts syndrome (RBS) (MIM #268300) is a rare, autosomal recessive disorder with prenatal and postnatal growth retardation, distinctive craniofacial abnormalities and limb defects; severely affected patients are unlikely to survive early childhood (1). The limb abnormalities of RBS are predominantly tetraphocomelia (symmetrical limb reduction). Other clinical features include mental retardation, cardiac and renal defects. Mutations in an evolutionarily conserved gene, *ESCO2,* are implicated in the aetiology of RBS (2-4). All RBS patients studied to date have biallelic mutations of the *ESCO2* gene. Of 26 mutations reported so far, all except one result in the complete or partial loss of the C-terminal acetytransferase domain of the ESCO2 protein (2,4). This domain is responsible for its canonical enzymatic activity. The ESCO2 gene resides on chromosome 8p21.1 and functions as a key regulator of a multi-protein complex known as cohesin (McKay et al., 1996; Toth et al., 1999; Vega et al., 2005), which is involved in multiple nuclear DNA transactions, including the establishment of sister chromatid cohesion during S-phase of the cell cycle, transcriptional regulation and DNA dsb repair. Although cohesin dysfunction has been implicated in cancer initiation and progression (5,6), cancer-proneness is not a feature of RBS, possibly because affected individuals die at an early age (http://www.omim.org).

It has been reported that some RBS patients' cells show hypersensitivity to DNA damaging agents causing DNA dsbs, such as ionizing radiation (IR) and mitomycin C (MMC) (7,8). Another study reported hypersensitivity of RBS fibroblasts to mitomycin C and camptothecin, but not to IR (9). In addition to the lack of agreement on cellular sensitivities to DNA damaging agents there is limited information on the molecular mechanisms underlying the limited DDR phenotypes described to date in RBS. We report here the first DDR analysis of a RBS family, *i.e.* including parents carrying *ESCO2* heterozygous mutations and provide evidence for penetrance of the cellular sensitivity to IR.

MATERIALS AND METHODS

Cell lines, DNA sequencing, and chromosome banding

Lymphoblastoid cell lines (LCLs) were established from peripheral blood mononuclear cells from the RSB-affected individual, her parents and a non-related control by Epstein-Barr Virus-transformation (10). Cells were maintained in RPMI-1640 medium, containing 20% fetal bovine serum (FBS) at 37^0C under 5% CO_2. Genomic DNA was extracted using a DNeasy Blood and Tissue Kit (Qiagen, USA). Mutation screens of *ESCO2* was performed by PCR amplification of all coding exons and intron-exon boundaries followed by Sanger sequencing with BigDye Terminator v3.1 cycle sequencing, and analyzed on an ABI 3730 (Applied Biosystems, USA). Chromosome banding was analysed the by Victorian Cytogenetic Services (Melbourne, Victoria, Australia).

Cell survival assay

Cell survival analyses were performed essential as described previously (11). Briefly, LCLs in exponentially growing phase from RSB-affected individual, parents and a non-related control were treated with IR or Mitomycin C (MMC). To determine radiosensitivity, cells were irradiated on ice with a graded dose of gamma radiation (0, 1, 2, and 3 Gy) from a ^{137}Cs source at a dose rate of 0.56 Gy per minute. Cell apoptosis was determined at 24 hr post -radiation by FACS analysis of sub-G1-phase cells. For survival analysis, cells were cultured for 96 hr, and cell viability was determined with a tetrazolinium salt WST-1 [2-(4-Iodophenyl)-3-(4-nitrophenyl)-5-(2,4-disulfophenyl)-2H-tetrazolium] (Roche Applied Science, Indianapolis, IN). The fraction of cell survival was expressed as a ratio of surviving cells to unirradiated cells. To determine MMC sensitivity, cells were treated with a graded dose of MMC (0, 0.1, 0.2, 0.3, 0.4 and 0.5 mM) for 24 hours. Following washing in phosphate buffered saline (PBS), cells were incubated at 37^0C under 5% CO_2 for 96 hr. Cell viability was determined as described above. Three independent experiments, each with four replicates, were performed for each data point. Survival curves were fitted by nonlinear regression analysis with the exponential model (Prism version 5.01, GraphPad Software, San Diego, California USA).

γ-H2AX focus analysis

γ-H2AX focus detection and analysis of DSB repair kinetics was performed as described (12). Briefly, cells in exponential phase of growth were washed twice with PBS and resuspended (0.7 million cells per ml of media) in fresh RPMI-1640 medium (Invitrogen) with 10% FBS. Cells were kept on ice for 10 mins and exposed to 0 and 2 Gy of gamma radiation from a ^{137}Cs source at a dose of 0.56Gy per minute. Cells were returned to 37^{0}C for 1 hr, 2 hr and 4 hr time points, whereas cells for the zero time point were processed for immunoflorescence (IF) staining immediately. For IF staining, 100 uL of cell suspension was dispensed onto polylysine slides (Menzel-Glaser, Germany) using a cytospin funnel, and spun at 500rpm for 5 minutes. Cells were fixed at room temperature (RT) for 5 minutes using 4% paraformaldehyde (Sigma-Aldrich, St Louis, MO, USA). Slides were washed twice with PBS, permeabilized in 0.1% Triton-X 100 and blocked with 1% BSA for 30 minutes at RT. Slides were then incubated for 2 hours at RT with anti-γ-H2AX mouse monoclonal antibody (1:500 dilution in 1% BSA, Merck, Germany). Following three washes in PBS, cells were incubated at RT for 1 hour with secondary antibody (Alexa-488 diluted 1:500 in PBS, Sigma-Aldrich). Cells were washed three times in PBS and DNA was stained using 4',6-diamidino-2-2-phenylindole (DAPI). Images were acquired using a x60 oil immersion objective on an Olympus IX81 microscope with Z-stage (Olympus, Japan) and Metamorph software for image acquisition and processing (Molecular Devices, CA, USA). Eight to ten Z-sections were acquired for each field and were deconvoluted for counting the foci. For each experiment, foci were counted in approximately 100 cells from 4 to 5 microscopy fields using a constant threshold value. Two independent experiments were analyzed except for the 2 hr time point.

Comet assay

Comet assay and analysis of dsb repair kinetics was performed as described previously (11). Briefly, LCLs were irradiated on ice with 8 Gy of gamma irradiation at a dose rate of 0.56 Gy per minute. Cells were harvested 0, 1 and 4 hr after irradiation. Unirradiated cells were used as a control for the basal level of DNA damage. The comet assay for the detection of DSBs was performed in neutral lysis buffer essentially as described (13). Cell lysis was performed in neutral lysis buffer (2M NaCl, 30 mM Na_2EDTA, 10 mM Tris-HCl, 1% Sarkosyl,

1% Triton X-100, and 10% DMSO [pH 8.3]), and electrophoresis was carried out in TBE buffer (2 mM Na_2EDTA, 90 mM Tris-HCl and 90 mM Boric acid [pH 8.3]). DNA damage was measured as the tail moment (tail moment = [(tail length × tail DNA intensity)/entire cell DNA intensity (head and tail)] × 100) with CASP image analysis software (http://casp.sourceforge.net). For each data point, eight to ten images were captured. Tail moments were measured for all cells, and doublets in each image were excluded. The mean of tail moment was calculated with a minimum of 50 cells per data point.

Sister chromatid break assays

Cells for sister chromatid break analysis were irradiated with 0.6 Gy from a ^{137}Cs source at a dose of 0.56Gy per minute on ice and allowed to recover at 37^0C for 30 min. Cells were incubated in colcemid (0.1□g/ml) at 37^0C for 60 min. Chromosome spreads were prepared as described previously (14). Chromatid and chromosome breaks were scored as described (15).

Western blot analysis, immunoprecipitations

Cells in the exponential phase of growth were exposed to 0 and 1 Gy of gamma radiation from a ^{137}Cs source at a dose of 0.56Gy per minute on ice. Cells were returned to 37^0C for 1 hr, 2 hr and 4 hrs, whereas cells for the t=0 time point were washed in PBS and proceeded to protein extraction immediately. For histone extraction, cells were lysed in PBS containing 0.5% Triton X 100, 2 mM PMSF and 0.02% NaN_3 10 min on ice, followed by centrifugation at 10,000 rpm for 1 minute at 4℃. Cells were incubated in extraction buffer (0.5N HCl + 10% glycerol) on ice for 30 minutes. Following centrifugation at 12,000 rpm for 5 minutes at 4℃, cell pellets were kept in acetone at –20℃ overnight. Following air-drying of the pellet, distilled water was added and protein concentration determined using the bicinchoninic acid assay (BCA assay) (Thermofisher Scientific). Western blot analyses were as described previously (5). Immunoprecipitation of ATM proteins was performed as described previously (16). Briefly, cell extracts were prepared by lysing cells for 45 min at 4 ℃ in ATM kinase lysis buffer containing 0.2% Tween 20, 1 mMNa_3VO_4, 1 mM NaF, 10 mMNa_2MoO_4, 20 mMβ-glycerophosphate, 5 μM microcystin-LR, 5 nM okadaic

acid, 5 µg/ml each of aprotinin, leupeptin, and pepstatin, 1 mM phenylmethylsulfonyl fluoride, and 1 mM dithiothreitol. Cell lysates were precleared in protein A/G-Sepharose, and used for immunoprecipitation with sheep polyclonal ATM antibodies overnight with constant mixing. Immune complexes were adsorbed onto protein G-Sepharose, washed, and resolved on SDS gels (5% acrylamide). After transfer to nitrocellulose membranes, they were probed consecutively with phospho-Ser^{367} ATM, phospho-Ser^{1981} ATM, and phospho-Ser^{1893} ATM antibodies with stripping between each step.

Statistical analysis

Analysis of cell survival was performed using regression analysis and statistical significance was analysed using the F-test (GraphPad Prism v5.01). For γ-H2AX focus and COMET analyses, paired Student t-Tests were performed.

RESULTS

The RBS family and ESCO2 mutation analysis

A female neonatal patient with a phenotype typical of RBS is presented. The affected individual had truncation of all limbs (**Figure 1A**), with bones distal to the flexures more severely affected. Toes and fingers were dysmorphic and the patient had a cleft lip and palate. The parents were phenotypically normal. The proband's chromosome analysis showed centromeric heterochromatin repulsion characteristic of, and confirming, the diagnosis of RBS (**Figures 1B-D**). Pathogenic compound heterozygous *ESCO2* mutations were identified in the patient. A c.760_761insA mutation (NM_001017420.2) predicting a truncating mutation p.(Thr254Asnfs*26) or p.(T254Nfs*26) in exon 3 and this mutation was identified in the father's blood sample (**Figure 1E**). A second mutation, c.1132-7A>G (NM_001017420.2), as predicted by three *in silico* programs MaxEntScan, NNSPLICE and Splice Site Finder (SSF) to change the splice acceptor site 7 bp downstream to create a cryptic splice acceptor site at the splice region of intron 6, resulting in an addition of one amino acid followed by a stop codon p.(Ile377_Asp378insLeu*) or p.(I377_D378insL*) (**Figure F and G**). This mutation was detected in the mother's blood sample (**Figure F and G**). RNA study confirmed the presence of aberrantly spliced transcripts in lymphocytes of the patient and the mother (**Figure H**). Both c.760_761insA and c.1132-7A>G mutations are present in the population at low frequencies of approximately 0.034% and 0.002% as recorded by gnomAD, and predict a truncated ESCO2 protein by approximately 57% and 37% resulting in loss of the acetyltransferase domain. The compound mutations have previously been reported in an Italian RBS family(2).

DNA damage response

After genotoxic trauma, mammalian cells exhibit a number of responses, including DNA repair, cell death and DNA damage checkpoint activation. We exposed LCLs derived from the patient, parents and a control individual to graded doses of IR, which induces DNA dsbs (and other DNA lesions), which are key mutagenic, clastogenic and lethal lesions induced by IR (17). The results showed significant reduction in survival of patient cells following IR, although not to the same extent as LCLs from a patient carrying homozygous mutations in the ATM gene, which were exquisitely IR-sensitive (**Figure 2A**). Cells from the heterozygous parents exhibited wild-type sensitivity to IR (**Figure**

2A). Likewise, treatment of LCLs with the DNA inter-strand cross-linking agent, MMC, also repaired at least partially by the DNA dsb repair machinery, resulted in a significantly reduced survival for patient cells ($p<0.05$)(**Figure 2B**).

We determined the susceptibility of the different cell lines to IR-induced cell death. Untreated cells from the patient and the father had significantly higher levels of apoptosis, suggesting their cellular instability (**Figure 2C**). Cells from the patient displayed a significant increase in apoptosis following a 2Gy dose of IR, which was most prominent at 24 hr (**Figure 2C**). Furthermore, patient cells exhibited a marked increase in sister chromatid breaks post 0.6 Gy IR (**Figure 2D**). Such a phenotype would be consistent with an inability to properly repair DNA dsbs. The latter phenotype was not evident in cells from the carriers (**Figure 2D**).

DNA damage checkpoints after IR

We next evaluated the ability of RBS patient cells to activate the DNA damage response following IR. DNA damage-induced phosphorylation of p53 at Ser15 was detected 1 hr post IR in patient cells, both parent cells and the control unaffected cells (**Figure 3A**). The p53S15 signal had largely diminished by 4 hr in the control and both heterozygous carriers, while it remained unchanged in patient cells (**Figure 3A**). The data are consistent with an adequate activation of the p53 checkpoint in RBS cells. Since p53 is phosphorylated at Ser15 by ATM (mutated in ataxia-telangiectasia) in response to IR (18), we determined whether ATM was activated in the patient's cells following IR. Previous reports have shown that autophosphorylation is associated with ATM's activation in human cells (19). Autophosphoration of ATM at three common sites, S367, S1893 and S1981, was evident in patient cells following IR (**Figure 3B**). Although a weaker signal of phosphorylated ATM in patient cells was observed, this is co-incident with a weaker signal on total immunoprecipitated ATM. Therefore, we considered that ATM activation is unlikely to be adversely affected in the patient cells. Likewise, ATM-mediated DNA damage-induced phosphorylation of cohesin SMC1A (an ATM phosphorylation target) at Ser957 was detected in the patient cells (**Figure 3C**). Together, the data suggest that these ESCO2 mutations have no apparent affect on the activation of the ATM-mediated DNA damage responses but that these cells are hypersensitive to agents that lead to DNA dsbs.

DNA dsb induction and repair

In view of their increased sensitivity to IR and MMC and IR-induced clastogenicity, we evaluated the ability of *ESCO2* mutant cells to repair IR-induced DNA damage, by determining the induction and repair of the γ-H2AX protein, which serves as a marker for dsbs (20-22), over three different time points post IR. On semi-quantitative Western blot analysis, an elevated level of γ-H2AX was detected 1 hr post IR in irradiated cells of all genotypes (**Figure 4A**). By 4 hr post IR, the signal intensity of γ-H2AX was significantly reduced in normal control and both parental heterozygous mutant cell lines. In contrast, the γ-H2AX signal persisted at a high level in patient cells (**Figure 4A**). These data suggest defective DNA dsb repair in the patient's cells, most of which ordinarily occurs by 4 hours post-induction (23,24).

Since heterozygous cells exhibited IR-induced γ-H2AX changes that were similar to *ESCO2* WT control cells, we focussed on the patient cells for subsequent assays. The kinetics of DNA dsb induction and repair was further evaluated by quantitative analyses of γ-H2AX foci following IR (**Figure 4B**). No statistically significant differences were detected in the basal level of γ-H2AX foci in unirradiated cells in any genotype. At 1 hr post IR, the typical and marked increase in the number of γ-H2AX foci was observed and this was followed by a decrease at 2 hr and 4 hr post IR in both patient and control cell lines (**Figure 4B**). Although the kinetics of γ-H2AX focus resolution were similar in patient and control cells, there were more residual γ-H2AX foci in patient cells, consistent with the γ-H2AX levels as detected on Western blots.

We further evaluated the potential DNA repair defect of RBS patient cells using the neutral 'comet' assay, which preferentially allows for the detection of DNA dsbs at the whole cell level (**Figure 4C**). RBS patient cells showed a significantly higher basal level of dsbs (**Figure 4D**), suggesting instability. Following IR, control cells exhibited a marked reduction in dsbs at 1 hr post IR; by 4 hr post IR, dsb quantities were comparable to the basal level. In contrast, dsbs remained at a high level in patient cells even after 4 hrs (**Figure 4E**).

DISCUSSION

Roberts Syndrome (RBS) is a rare, recessively-inherited genetic disorder. Its canonical clinical features include growth retardation, truncation of the limbs and craniofacial abnormalities. A number of Mendelian disorders manifest the latter characteristic, along with clinical or *in vitro* radiosensitivity (Table 1). These disorders are characterized in most cases by autosomal recessive inheritance and by structural or functional facial abnormalities. Many different genes are responsible.

Here we report for the first time, the characterization of the cellular DNA damage response (DDR) in a RBS kindred. Our affected case showed the typical clinical and cytogenetic features (Figure 1) characteristic of the disorder. We demonstrated that mutations affecting the acetyltransferase domain of the *ESCO2* gene present in the patient were inherited from her parents. The affected individual manifested multiple cellular abnormalities of the DDR.

The first mammalian components of the cohesin complex were discovered over two decades ago (24). Cohesin proteins have major roles in a number of fundamental molecular processes, including sister chromatid cohesion, transcriptional control and DNA dsb repair. In recombinational repair of DNA dsbs, there is genetic and biochemical evidence from multiple species that cohesin accumulates around the site of the dsb and stabilizes it for subsequent enzymatic activity by homologous recombination enzymes (25-28). Cohesin is a multiprotein complex with four core components: RAD21, SMC1 (structural maintenance of chromatin 1), SMC3 and an SA (stromal antigen) subunit (either SA1, SA2 or SA3); numerous cohesin-associated and cohesin-regulator proteins are now known, including ESCO2 (29).

Transfer of an acetyl group is important for various protein-protein interactions. The acetyltransferase activity of the ESCO2 protein is required for the acetylation of the core cohesin component SMC3 (30). This has been shown to be essential for the localization of cohesin to chromosomes (pericentric heterochromatin) (31) and for the establishment of sister chromatid cohesion during DNA replication (32).

We characterized DDRs in a RBS-affected family. The RBS-affected individual showed clear evidence of chromosomal instability and increased sensitivity to IR and mitomycin-C. This finding is consistent with a previous report of increased sensitivity to DNA damaging agents, including IR, in fibroblasts derived from RBS patients (7), but differed from another report, which demonstrated that RBS cells were sensitive to several DNA damaging agents,

failed to show their sensitivity to IR (8). It is possible that the genotoxin-sensitivity phenotype is mutation-dependent. Also, mutations in RAD21, a member of the cohesin complex, led to chromosomal aberrations and radiosensitivity in humans (11) and genetically engineered mice (14). In addition, reducing cohesin levels had a greater impact on chromosome condensation, repetitive DNA stability and DNA repair compared to that on sister-chromatid cohesion and chromosome segregation (33). A lack of cohesin in meiosis leads to the accumulation of deleterious DNA dsbs (34). Collectively, these data support a role for the cohesin complex and its regulators in DNA (dsb) repair.

The work described here strongly suggests that the cells of the ESCO2 homozygous patient are defective in DNA dsb repair. This was shown directly in multiple assays, including chromosome/chromatid break assay, γH2AX Western blots and immunofluorescence and neutral comet assay, and indirectly with IR and MMC-clonogenic survival. Increased sensitivity to IR of the RBS cells did not appear to be due to a defect in ATM activation or signaling through its downstream substrates.

Our data suggest that the acetyltransferase activity of ESCO2 is likely required for the repair of DNA dsbs. Since cohesin loading to the sites of DNA breaks is required for efficient DNA repair, the observed DNA repair defect in RBS–affected cells is likely due to a defective function of ESCO2 in facilitating cohesin loading onto chromatin following DNA damage.

In addition to its developmental features, RBS can hence be considered a disorder of the DDR, including defective repair of DNA dsbs. The affected gene, ESCO2, is a DDR gene at a number of levels, and specifically, a new addition to the list of human DNA dsb repair genes.

ACKNOWLEDGEMENT

We thank the NHMRC of Australia for Project Grants to HX/MJM/RGR/JC/PK/MFL and SK. We acknowledge the microscopy core at the Peter MacCallum Cancer Centre.

FIGURE LEGENDS

Figure 1. **A.** The RBS patient. **B-D.** Representative metaphase chromosome spreads from the RBS patient, exhibiting characteristic heterochromatin splaying / repulsion (arrowed and one example in each enlarged) on solid-stained **B**, G-banded **C** and C-banded spreads **D**, **E, F.** DNA chromatograph of mutations detected in mother, father and proband. **G.** Predicted change of the acceptor site by the c.1132-7A>G mutation. D. Asparatic acid; A. Alanine; X. Stop codon. L. Leucine. **H.** PCR detection of aberrantly spliced transcripts in RNA from lymphocytes of mother and proband but not in the control.

Figure 2. Genotoxin sensitivity of cells from the different RBS genotypes. 'AT-cells' are from an ataxia-telangiectasia compound heterozygote. LCLs of the different genotypes treated with graded doses of IR (**A**), or with MMC (**B**), three independent replicate experiments for each cell line. **C**. IR-induced apoptosis, duplicate experiments for each cell line. Each cell line was subjected to 2Gy and resulting apoptosis % determined. **D**. Low-dose (0.6Gy) IR-induced clastogenicity. Arrows show sister chromatid breaks. Sb, sister chromatid breaks; Cb, chromosome breaks; Int, interchanges; ICA, induced chromosome aberrations/metaphase. Duplicate experiments.

Figure 3. Activation of cell cycle checkpoints in RBS and control cells after IR exposures. **A**. p53 serine 15 phosphorylation after 2Gy IR to cells of the four genotypes. *Top panel*: anti-p53, serine 15. *Bottom panel*: anti-pan actin control. **B**. ATM activation at various phosphorylation sites in RBS and control cells after 3Gy IR. *Top panel*: ATM phosphorylation sites S367, S1893 and S1981 were examined with or without IR. C2: control 2. *Bottom panel*: Loading control: sheep IgH. **C**. SMC1A cohesin phosphorylation in RBS cells after 3Gy IR. *Bottom panel*: Total SMC1A protein lane loading. Images are representative of at least duplicate experiments.

Figure 4. Kinetics of induction and repair of DNA dsbs in RBS cells after ionizing radiation. **A**. γ-H2AX levels in control and RBS cells after 1Gy ionizing radiation, as assayed by Western blot analysis. Histone 3 was a loading control. **B**. Appearance and time-course of γ-H2AX foci in control and RBS cells after IR. **C**. 'Comet' assay showing unirradiated and irradiated (+6Gy) cells. Damaged DNA (tail) was quantitated relative to

intact DNA (head). **D** and **E**. Quantitation of DNA dsbs at the basal level (**D**) (* $p<0.05$.) and post IR (**E**). Images and graphs are representative of at least duplicate experiments.

REFERENCES

1. Roberts, J. B. (1919). A child with double cleft lip and palate, protrusion of the intermaxillary portion of the upper jaw and imperfect development of the bones of the four extremities. Ann Surg *70*, 252-253.

2. Gordillo, M., Vega, H., Trainer, A. H., Hou, F., Sakai, N., Luque, R., Kayserili, H., Basaran, S., Skovby, F., Hennekam, R. C.*, et al.* (2008). The molecular mechanism underlying Roberts syndrome involves loss of ESCO2 acetyltransferase activity. Hum Mol Genet *17*, 2172-2180.

3. Vega, H., Waisfisz, Q., Gordillo, M., Sakai, N., Yanagihara, I., Yamada, M., van Gosliga, D., Kayserili, H., Xu, C., Ozono, K.*, et al.* (2005). Roberts syndrome is caused by mutations in ESCO2, a human homolog of yeast ECO1 that is essential for the establishment of sister chromatid cohesion. Nat Genet *37*, 468-470.

4. Vega, H., Trainer, A. H., Gordillo, M., Crosier, M., Kayserili, H., Skovby, F., Uzielli, M. L., Schnur, R. E., Manouvrier, S., Blair, E.*, et al.* (2010). Phenotypic variability in 49 cases of ESCO2 mutations, including novel missense and codon deletion in the acetyltransferase domain, correlates with ESCO2 expression and establishes the clinical criteria for Roberts syndrome. J Med Genet *47*, 30-37.

5. **Xu H**, Yan Y, Deb S, et al, Cohesin Rad21 mediates loss of heterozygosity and is upregulated via Wnt promoting transcriptional dysregulation in gastrointestinal tumors. Cell Reports, 2014;9:1781-1797.

6. **Xu H**, Tomaszewski JM, **McKay MJ**. Can corruption of chromosome cohesion create a conduit to cancer? Nat Rev Cancer, 2011;11:199-210.

7. Allingham-Hawkins, D. J., and Tomkins, D. J. (1995). Heterogeneity in Roberts syndrome. Am J Med Genet *55*, 188-194.

8. Van den Berg, D. J., and Francke, U. (1993). Sensitivity of Roberts syndrome cells to gamma radiation, mitomycin C, and protein synthesis inhibitors. Somat Cell Mol Genet *19*, 377-392.

9. van der Lelij P, Godthelp BC, van Zon W, van Gosliga D, Oostra AB, Steltenpool J, de Groot J, Scheper RJ, Wolthuis RM, Waisfisz Q, Darroudi F, Joenje H, de Winter JP.The cellular phenotype of Roberts syndrome fibroblasts as revealed by ectopic expression of ESCO2. PLoS One. 2009;4:e6936.

10. Tosato, G., and Cohen, J. I. (2007). Generation of Epstein-Barr Virus (EBV)-immortalized B cell lines. Curr Protoc Immunol *Chapter 7*, Unit 722.

11. Deardorff, M. A., Wilde, J. J., Albrecht, M., Dickinson, E., Tennstedt, S., Braunholz, D., Monnich, M., Yan, Y., Xu, W., Gil-Rodriguez, M. C.*, et al.* (2012). RAD21 mutations cause a human cohesinopathy. Am J Hum Genet *90*, 1014-1027.

12. Vasireddy, R. S., Sprung, C. N., Cempaka, N. L., Chao, M., and McKay, M. J. (2010). H2AX phosphorylation screen of cells from radiosensitive cancer patients reveals a novel DNA double-strand break repair cellular phenotype. Br J Cancer *102*, 1511-1518.

13. Wojewódzka M, Buraczewska I, Kruszewski M. A modified neutral comet assay: elimination of lysis at high temperature and validation of the assay with anti-single-stranded DNA antibody. Mutat Res. 2002;518:9-20.

14. Xu, H., Balakrishnan, K., Malaterre, J., Beasley, M., Yan, Y., Essers, J., Appeldoorn, E., Thomaszewski, J. M., Vazquez, M., Verschoor, S.*, et al.* (2010). Rad21-cohesin haploinsufficiency impedes DNA repair and enhances gastrointestinal radiosensitivity in mice. PLoS One *5*: e12112.

15. Price, F. M., Parshad, R., Tarone, R. E., and Sanford, K. K. (1991). Radiation-induced chromatid aberrations in Cockayne syndrome and xeroderma

pigmentosum group C fibroblasts in relation to cancer predisposition. Cancer Genet Cytogenet *57*, 1-10.

16. Kozlov, S. V., Graham, M. E., Jakob, B., Tobias, F., Kijas, A. W., Tanuji, M., Chen, P., Robinson, P. J., Taucher-Scholz, G., Suzuki, K.*, et al.* (2011). Autophosphorylation and ATM activation: additional sites add to the complexity. J Biol Chem *286*, 9107-9119.

17. Shibata, A., and Jeggo, P. A. (2014). DNA double-strand break repair in a cellular context. Clin Oncol (R Coll Radiol) *26*, 243-249.

18. Khanna, K. K., Keating, K. E., Kozlov, S., Scott, S., Gatei, M., Hobson, K., Taya, Y., Gabrielli, B., Chan, D., Lees-Miller, S. P., and Lavin, M. F. (1998). ATM associates with and phosphorylates p53: mapping the region of interaction. Nat Genet *20*, 398-400.

19. Lavin, M. F., Delia, D., and Chessa, L. (2006). ATM and the DNA damage response. Workshop on ataxia-telangiectasia and related syndromes. EMBO Rep *7*, 154-160.

20. Scully R, Xie A. Double strand break repair functions of histone H2AX. Mutat Res. 2013 Oct;750(1-2):5-14

21. Valdiglesias V, Giunta S, Fenech M, Neri M, Bonassi S. γH2AX as a marker of DNA double strand breaks and genomic instability in human population studies. Mutat Res. 2013;753:24-40.

22. Royba, E., Miyamoto, T., Natsuko Akutsu, S., Hosoba, K., Tauchi, H., Kudo, Y., Tashiro, S., Yamamoto, T., and Matsuura, S. (2017). Evaluation of ATM heterozygous mutations underlying individual differences in radiosensitivity using genome editing in human cultured cells. Sci Rep *7*, 5996.

23. McKay, M. J., and Kefford, R. F. (1995). The spectrum of in vitro radiosensitivity in four human melanoma cell lines is not accounted for by

differential induction or rejoining of DNA double strand breaks. Int J Radiat Oncol Biol Phys *31*, 345-352.

24. Pouliliou, S., and Koukourakis, M. I. (2014). Gamma histone 2AX (gamma-H2AX)as a predictive tool in radiation oncology. Biomarkers *19*, 167-180.
25. Litwin I, Wysocki R. New insights into cohesin loading. Curr Genet. 2018;64:53-61.

25. McKay, M. J., Troelstra, C., van der Spek, P., Kanaar, R., Smit, B., Hagemeijer, A., Bootsma, D., and Hoeijmakers, J. H. (1996). Sequence conservation of the rad21 Schizosaccharomyces pombe DNA double-strand break repair gene in human and mouse. Genomics *36*, 305-315.

26. Kong X, Ball AR Jr, Yokomori K. The Use of Laser Microirradiation to Investigate the Roles of Cohesins in DNA Repair. Methods Mol Biol. 2017;1515:227-242.

27. Ding DQ, Haraguchi T, Hiraoka Y. A cohesin-based structural platform supporting homologous chromosome pairing in meiosis. Curr Genet. 2016;62:499-502.

28. Mehta GD, Kumar R, Srivastava S, Ghosh SK. Cohesin: functions beyond sister chromatid cohesion. FEBS Lett. 2013;587:2299-312.

29. Dorsett, D. (2011). Cohesin: genomic insights into controlling gene transcription and development. Curr Opin Genet Dev *21*, 199-206.

30. Whelan, G., Kreidl, E., Peters, J. M., and Eichele, G. (2012a). The non-redundant function of cohesin acetyltransferase Esco2: some answers and new questions. Nucleus *3*, 330-334.

31. Whelan, G., Kreidl, E., Wutz, G., Egner, A., Peters, J. M., and Eichele, G. (2012b). Cohesin acetyltransferase Esco2 is a cell viability factor and is required for cohesion in pericentric heterochromatin. EMBO J *31*, 71-82.

32. Terret, M. E., Sherwood, R., Rahman, S., Qin, J., and Jallepalli, P. V. (2009). Cohesin acetylation speeds the replication fork. Nature *462*, 231-234.

33. Heidinger-Pauli, J. M., Unal, E., Guacci, V., and Koshland, D. (2008). The kleisin subunit of cohesin dictates damage-induced cohesion. Mol Cell *31*, 47-56.

34. Nambiar M, Smith GR. Pericentromere Specific Cohesin Complex Prevents Meiotic Pericentric DNA Double-Strand Breaks and Lethal Crossovers. Mol Cell. 2018; 16;71:540-553.

Table 1. Human syndromes characterized by facial abnormalities and radiosensitivity.

Syndrome	Gene	Locus	Inheritance	Facial features
Roberts	ESCO2	8p21.1	Recessive	Cleft palate and lip
Ataxia-telangiectasia	ATM	11q22.3	Recessive	Choreiform facial movements; Dysarthric speech; Ocular telangiectasia
Ataxia-telangiectasia -Like	MRE11	11q21	Recessive	Dysarthric speech; Ocular telangiectasia
RIDDLE	RNF168	3q29	Recessive	Facial dysmorphism; Ocular telangiectasia
Ligase IV	LIGIV	13q33.3	Recessive	Facial dysmorphism
Nijmegen Breakage	NBS1	8q21.3	Recessive	Choreiform facial movements; Dysarthric speech; Ocular telangiectasia
Ataxia, adult onset, with oculomotor apraxia	APTX	9p21.1	Recessive	Choreiform facial movements; oculomotor apraxia
Basal cell naevus	PTCH1, PTCH2, SUFU	9q22.32, 1p24.1, 10q24.32	Dominant	Broad facies; Frontal bossing; Mandibular prognathism; Odontogenic keratocysts of jaws; Strabismus; Lateral displacement of the inner canthi; Hypertelorism; Iris coloboma; Broad nasal root; Cleft lip and palate

Data from Online Mendelian Inheritance in Man (https://www.omim.org/).

Figure 1

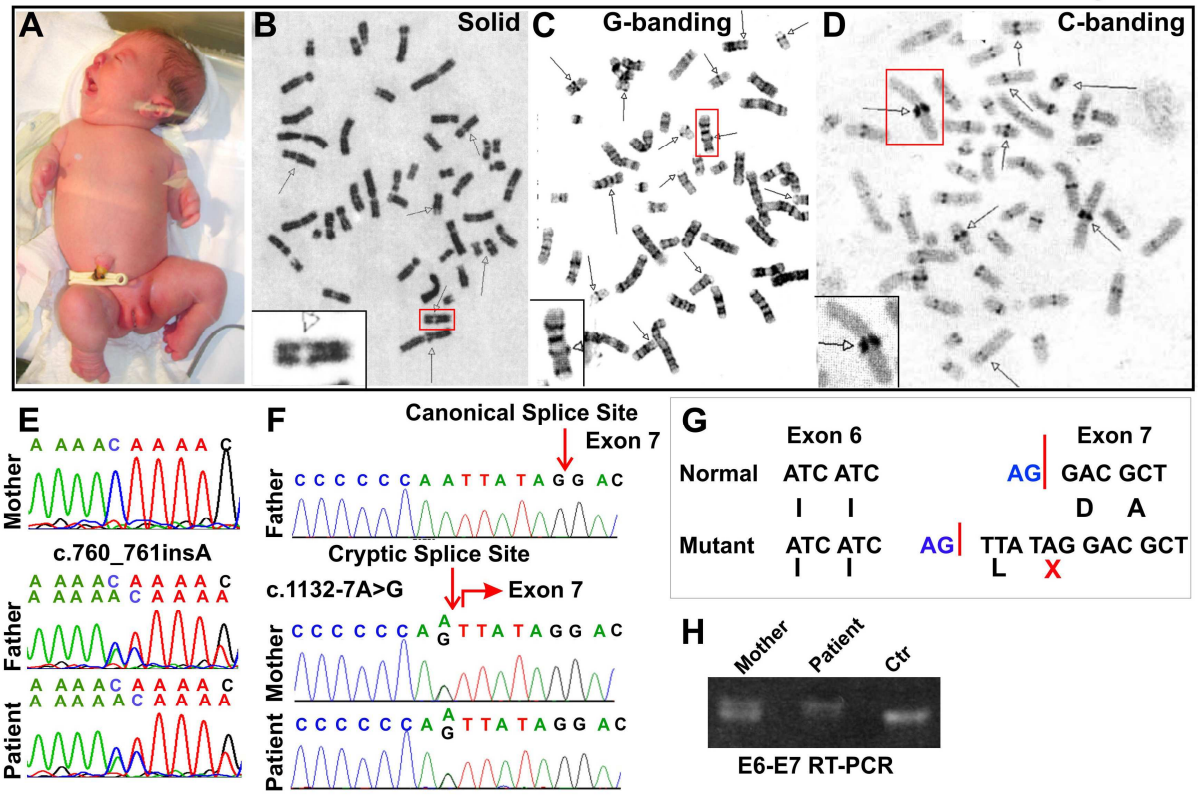

Figure 2

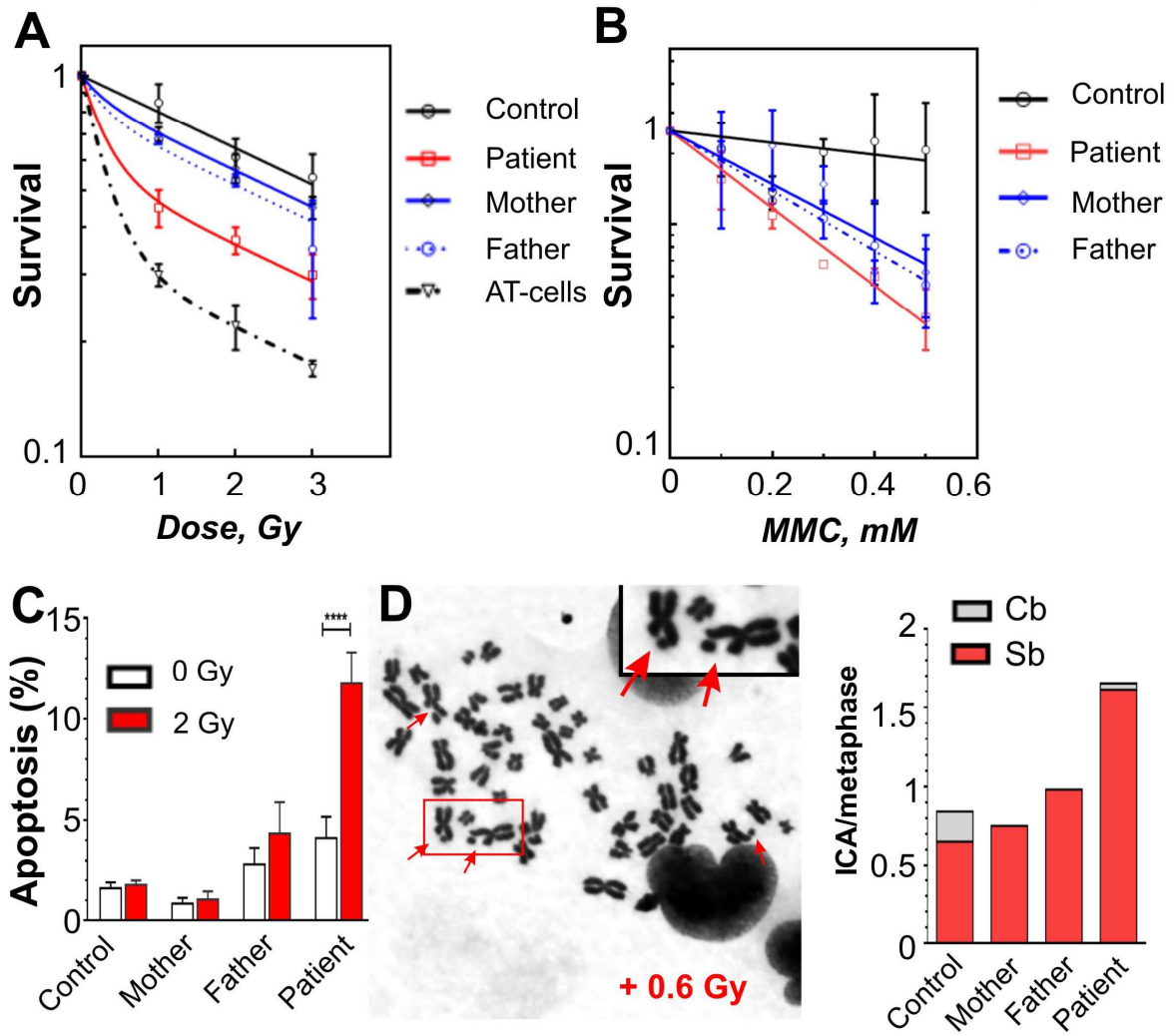

Figure 3

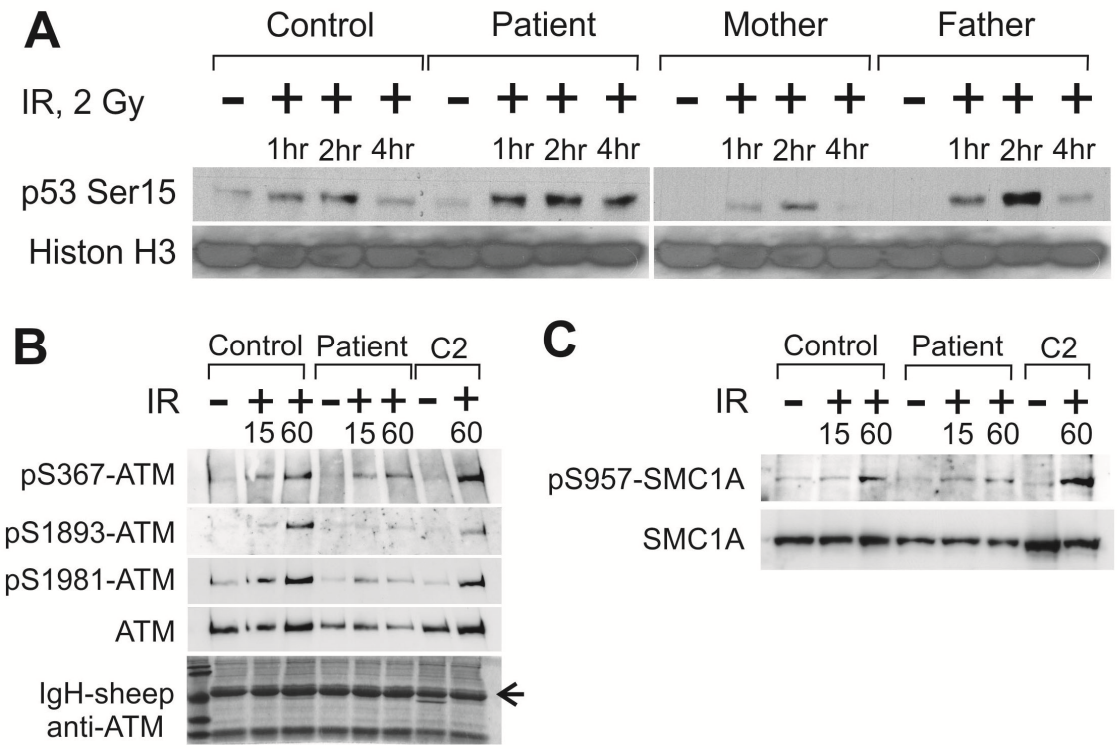

Figure 4

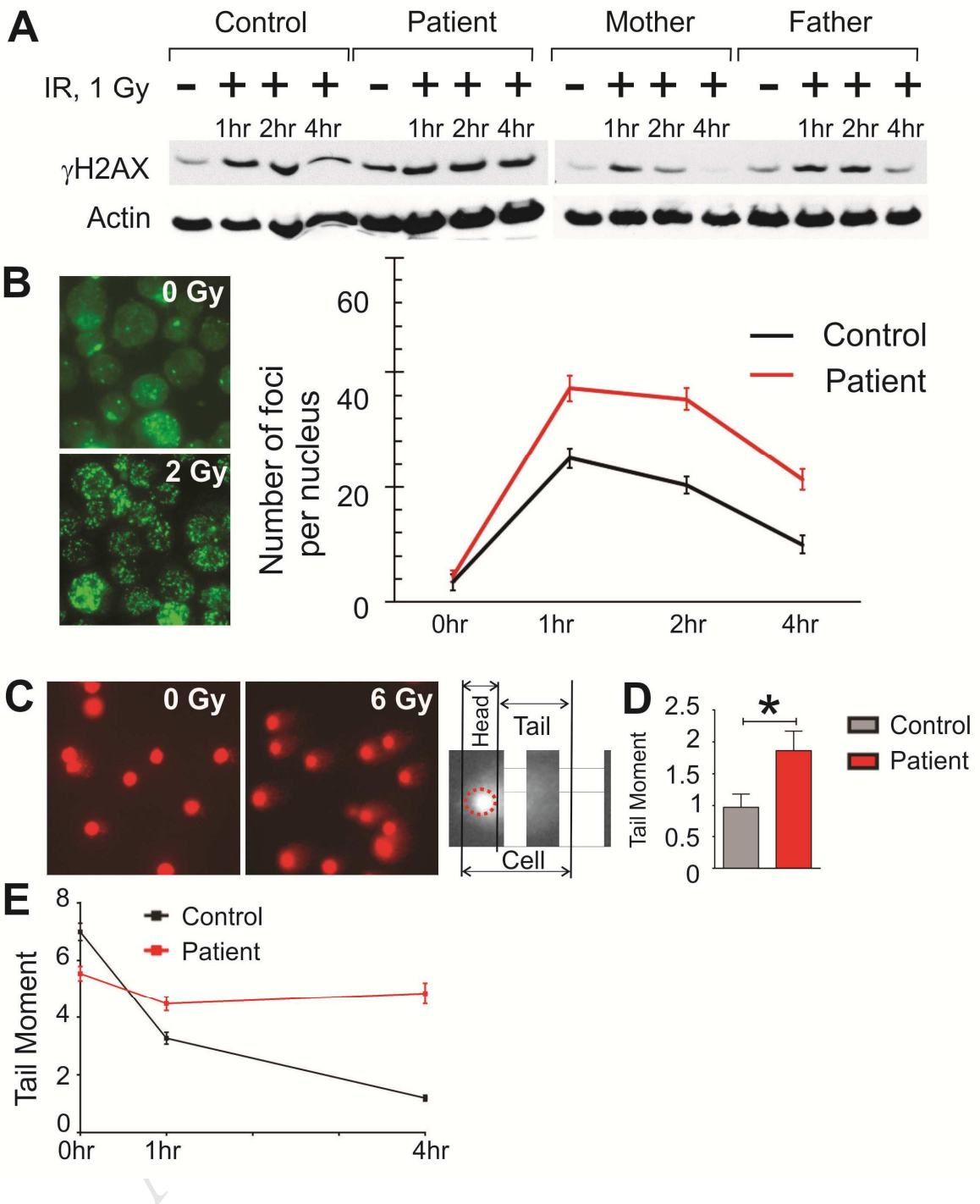
A
Control
Patient
Mother
Father
IR, 1 Gy
- + + + - + + + - + + + - + + +
1hr 2hr 4hr 1hr 2hr 4hr 1hr 2hr 4hr 1hr 2hr 4hr
γH2AX
Actin
B
0 Gy
2 Gy
Number of foci per nucleus
60
40
20
0
0hr
1hr
2hr
4hr
Control
Patient
C
0 Gy
6 Gy
Head
Tail
Cell
D
Tail Moment
2.5
2
1.5
1
0.5
0
*
Control
Patient
E
Tail Moment
8
6
4
2
0
0hr
1hr
4hr
Control
Patient